Chemical Science

ROYAL SOCIETY OF CHEMISTRY

EDGE ARTICLE

View Article Online
View Journal | View Issue

Cite this: *Chem. Sci.*, 2023, **14**, 12091

All publication charges for this article have been paid for by the Royal Society of Chemistry

Received 17th July 2023
Accepted 4th October 2023

DOI: 10.1039/d3sc03686c

rsc.li/chemical-science

Organocatalytic atroposelective synthesis of axially chiral *N,N′*-pyrrolylindoles *via de novo* indole formation†

Cong-Shuai Wang,‡[ab] Qi Xiong,‡[a] Hui Xu,‡[c] Hao-Ran Yang,[a] Yanfeng Dang,*[c] Xiu-Qin Dong*[a] and Chun-Jiang Wang*[ab]

The first organocatalytic atroposelective synthesis of axially chiral *N,N′*-pyrrolylindoles based on *o*-alkynylanilines was successfully established *via de novo* indole formation catalyzed by chiral phosphoric acid (CPA). This new synthetic strategy introduced CPA-catalyzed asymmetric 5-*endo*-*dig* cyclization of new well-designed *o*-alkynylanilines containing a pyrrolyl unit, resulting in a wide range of axially chiral *N,N′*-pyrrolylindoles in high yields with exclusive regioselectivity and excellent enantioselectivity (up to 99% yield, >20 : 1 rr, 95 : 5 er). Considering the potential biological significance of N–N atropisomers, preliminary biological activity studies were performed and revealed that these structurally important *N,N′*-pyrrolylindoles had a low IC_{50} value with promising impressive cytotoxicity against several kinds of cancer cell lines. DFT studies reveal that the *N*-nucleophilic cyclization mediated by CPA is the rate- and stereo-determining step, in which ligand–substrate dispersion interactions facilitate the axial chirality of the target products.

Introduction

N–N atropisomers are widely present as core structures in a variety of important chiral molecules, such as natural products, chiral ligands and functional materials (Scheme 1a).[1] In sharp contrast to the well-developed syntheses of C–C and C–N axially chiral compounds,[2] the construction of N–N atropisomers has remained in an underdeveloped state in the decades since their discovery in 1931.[3] The asymmetric catalytic synthesis of N–N axially chiral compounds was considered a challenging issue until 2021, when Li,[4a] Lu and Houk,[4b] and Liu's[5a] groups developed various synthetic methods to access these fascinating molecules promoted by chiral transition metals or organocatalysis.

Subsequently, a great deal of attention has been paid to the development of efficient synthetic strategies and some progress has been achieved, mainly involving direct N–H functionalization,[4] the functionalization of prochiral or racemic bis-heteroaryl rings,[5] *de novo* ring formation *via* a Paal–Knorr reaction,[6] or dual-ring formation by cyclization and oxidation.[7]

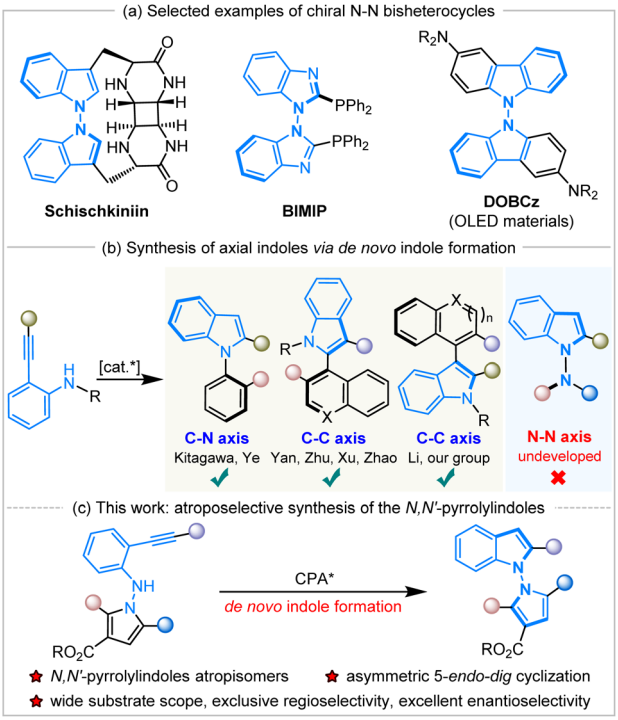

Scheme 1 Selected examples of N–N atropisomers and asymmetric *de novo* construction of indole atropisomers.

[a]*College of Chemistry and Molecular Sciences, Engineering Research Center of Organosilicon Compounds & Materials, Ministry of Education, Wuhan University, Wuhan, Hubei, 430072, P. R. China. E-mail: xiuqindong@whu.edu.cn*

[b]*State Key Laboratory of Elemento-organic Chemistry, Nankai University, Tianjin, 300071, China. E-mail: cjwang@whu.edu.cn*

[c]*Tianjin Key Laboratory of Molecular Optoelectronic Sciences, Department of Chemistry, Tianjin University, Tianjin, 300072, China. E-mail: yanfeng.dang@tju.edu.cn*

† Electronic supplementary information (ESI) available. CCDC 2279386. For ESI and crystallographic data in CIF or other electronic format see DOI: https://doi.org/10.1039/d3sc03686c

‡ These authors contributed equally.

In addition, the catalytic atroposelective synthesis of N–N axially chiral molecules *via de novo* indole formation has emerged as an attractive route.[8] The 5-*endo-dig* cyclization of *o*-alkynylanilines is a versatile method for the *de novo* generation of indole derivatives, and a variety of chiral indole atropisomers[9] have been well established through this catalytic enantioselective cyclization (Scheme 1b). To our knowledge, the documented protocols rely heavily on asymmetric transition metal catalysis, and there are only two examples using organocatalysis for the construction of axially chiral indoles *via* the 5-*endo-dig* cyclization of *o*-alkynylanilines. In 2019, Yan and workers developed chiral quinine-derived thiourea-catalyzed asymmetric cyclization of *o*-alkynylanilines to give chiral naphthyl-C2-indoles with a C–C axis *via* vinylidene orthoquinone methide intermediates with excellent results.[9c] Meanwhile, Ye and coworkers realized chiral CPA-catalyzed atroposelective 5-*endo-dig* cyclization of ynamides to access chiral *N*-arylindoles with a C–N axis in high yields with excellent enantioselectivities.[9d] However, the approach to accessing axially chiral N–N bis-heteroaryl atropisomers through the *de novo* formation of chiral indole rings by the organocatalytic annulation of *o*-alkynylanilines remains undeveloped and unprecedented. During the preparation of this manuscript, Sparr and coworkers reported an asymmetric Pd-catalyzed 5-*endo*-hydroaminocyclization for the synthesis of N–N atropisomeric bisindoles and indolyl-carbazoles with moderate results.[9j]

Herein, we have designed and synthesized a new type of molecule, *N*-pyrrole *o*-alkynylanilines, as the substrates, and applied them in Brønsted-acid CPA-catalyzed atroposelective 5-*endo-dig* cyclization to achieve the *de novo* formation of axially chiral *N*,*N*′-pyrrolylindoles (Scheme 1c). It should be noted that this is the first organocatalytic annulation of *o*-alkynylanilines to prepare N–N axially chiral compounds in a practical and atom-economic manner. This fascinating protocol also faces a lot of challenges, including: (1) the development of new and efficient synthetic strategies to access N–N axially chiral molecules with excellent enantioselective control, (2) the design and synthesis of new kind of substrates and chiral N–N bis-heteroaryl pyrrolylindoles atropisomers, (3) the discovery and application of these highly-valuable molecules in the field of synthetic and medicinal chemistry.

Results and discussion

Optimization of reaction conditions

To verify this hypothesis, an initial investigation of the asymmetric 5-*endo-dig*-cyclization was begun with *N*-pyrrolo-acetylaniline **1a** as the model substrate promoted by chiral phosphoric acids. A series of BINOL-based chiral phosphoric acids **CPA1–CPA8** as the catalysts were firstly applied to promote this cyclization in $CHCl_3$. Except for **CPA3** with a 1-naphthyl group, the formation of the expected **2a** with an N–N axis could be obtained in high yields but with poor enantioselectivity (Table 1, entries 1–8). H_8-BINOL-based chiral phosphoric acids **CPA9–CPA10** were also employed but, unfortunately, no further improvement was obtained (Table 1, entries 9 and 10). We found that SPINOL-derived **CPA11–CPA14** could promote smooth cyclization, and the desired products could be obtained with better results (90–96% yields, 74 : 26–89 : 11 er, Table 1, entries 11–14). Pleasingly, SPINOL-derived **CPA12** containing a 1-pyrenyl substituted group furnished the best results in terms of reactivity and enantioselectivity (93% yield, 89 : 11 er, Table 1, entry 12). A further solvent survey in the presence of **CPA12** revealed that toluene is the most favorable choice, and the enantioselectivity of product **2a** was greatly improved to 91 : 9 er (Table 1, entry 19). When the reaction temperature was gradually decreased to −10 °C, excellent enantioselectivity was obtained (90% yield, 95 : 5 er, Table 1, entry 22). It was found that the ee value was maintained without improvement at −40 °C, but lower reactivity was observed with only 50% yield (Table 1, entry 23). Accordingly, it was identified that the optimized protocol for the 5-*endo-dig*-cyclization of *N*-pyrrolo-acetylanilines should be conducted under conditions with SPINOL-derived **CPA12** as the privileged catalyst in toluene at −10 °C.

Substrate scope study

With the established optimal conditions in hand, we focused on an evaluation of the substrate generality of *N*-pyrrolo-acetylanilines for this **CPA12**-catalyzed 5-*endo-dig*-cyclization. As summarized in Table 2, a wide range of *N*-pyrrolo-acetylanilines with different substituted groups on the phenyl ring and indole ring were applied to prepare chiral pyrrolyindoles containing an N–N axis. It was found that the electronic properties and positions of the substituted groups have a negligible impact on the reactivity and enantioselectivity. The *N*-pyrrolo-acetylanilines bearing electron-rich (**1b–1d**) or electron-deficient (**1e**) groups on the indole ring were examined first, and the expected annulation products (**2b–2e**) were furnished in 87–97% yields with 91 : 9–95 : 5 er. In addition, the *N*-pyrrolo-acetylanilines (**1f–1j**) containing different substituted groups on the phenyl ring of the aniline motifs could be well accommodated to give the desired products (**2f–2j**) in good to high yields with excellent enantioselectivities (81–97% yields, 91 : 9–95 : 5 er). The absolute configuration of cycloadduct **2b** was unambiguously determined as *S* by X-ray diffraction analysis (CCDC 2279386).[10]

On the other hand, we also investigated the feasibility of the **CPA12**-catalyzed 5-*endo-dig*-cyclization of *N*-pyrrolo-acetylanilines with different substituted groups on the phenyl ring in the pyrrole motif. It was found that a wide range of *N*-pyrrolo-acetylanilines (**1k–1t**) bearing electron-rich groups or electron-deficient groups on the phenyl ring worked as good reaction partners, and this cyclization proceeded smoothly, resulting in the corresponding chiral products (**2k–2t**) in good to high yields with excellent enantioselectivities (87–96% yields, 87 : 13–95 : 5 er). It is noteworthy that the position of the substituted group did not affect the reactivity or enantioselectivity. Additionally, the heteroaryl-fused substrate **1u** was well tolerated to deliver the corresponding product **2u** in 90% yield with 90 : 10 er. Remarkably, the alkyl-substituted substrate **1v** also worked well, leading to the expected product **2v** in high yield with good enantioselectivity (97% yield, 95 : 5 er) (Table 3).

Table 1 Optimization of reaction conditions[a]

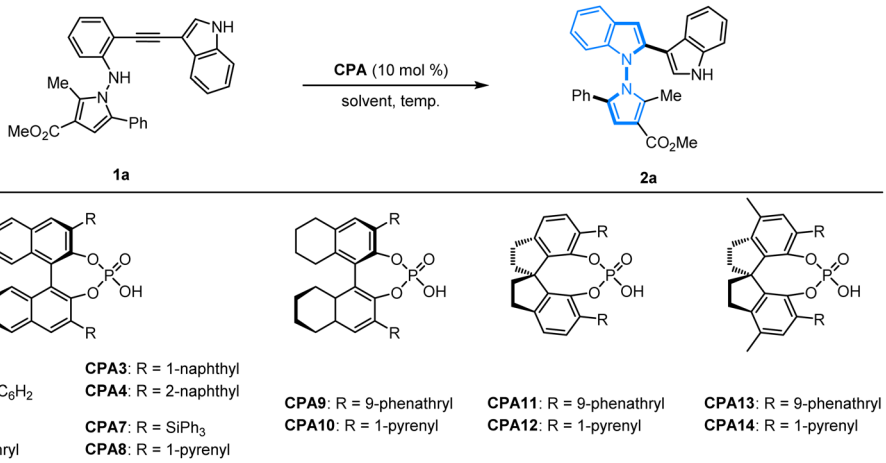

Entry	CPA	Solvent	T (°C)	Yield[b] (%)	ee[c] (%)
1	(*R*)-**CPA1**	$CHCl_3$	RT	96	50 : 50
2	(*R*)-**CPA2**	$CHCl_3$	RT	95	54 : 45
3	(*R*)-**CPA3**	$CHCl_3$	RT	Trace	—
4	(*R*)-**CPA4**	$CHCl_3$	RT	93	50 : 50
5	(*R*)-**CPA5**	$CHCl_3$	RT	95	50 : 50
6	(*R*)-**CPA6**	$CHCl_3$	RT	96	61 : 39
7	(*R*)-**CPA7**	$CHCl_3$	RT	90	50 : 50
8	(*R*)-**CPA8**	$CHCl_3$	RT	90	69 : 31
9	(*R*)-**CPA9**	$CHCl_3$	RT	95	65 : 35
10	(*R*)-**CPA10**	$CHCl_3$	RT	Trace	—
11	(*S*)-**CPA11**	$CHCl_3$	RT	90	76 : 24
12	(*S*)-**CPA12**	$CHCl_3$	RT	93	89 : 11
13	(*S*)-**CPA13**	$CHCl_3$	RT	94	74 : 26
14	(*S*)-**CPA14**	$CHCl_3$	RT	96	84 : 16
15	(*S*)-**CPA12**	EtOAc	RT	Trace	—
16	(*S*)-**CPA12**	THF	RT	Trace	—
17	(*S*)-**CPA12**	CH_3CN	RT	92	60 : 40
18	(*S*)-**CPA12**	Acetone	RT	Trace	—
19	(*S*)-**CPA12**	Toluene	RT	95	91 : 9
20	(*S*)-**CPA12**	Toluene	10	95	92 : 8
21	(*S*)-**CPA12**	Toluene	0	93	93 : 7
22	(*S*)-**CPA12**	Toluene	−10	90	95 : 5
23	(*S*)-**CPA12**	Toluene	−40	50	95 : 5

[a] All reactions were carried out with 0.2 mmol **1a** in 2 mL of solvent catalyzed by **CPA** (10 mol%). [b] Isolated yield of the two steps overall. [c] The er value was determined by chiral HPLC analysis.

Scale-up experiments and synthetic applications

The configurational stability of the novel axially chiral N–N biheteroaryl pyrrolylindoles was investigated, and no erosion of enantiopurity was observed when the product **2a** was heated in toluene at 130 °C for 48 h. Therefore, the configurational stability of these compounds could certainly show good tolerance for their further application in organic synthesis. To further highlight the application of this protocol for the synthesis of novel axially chiral biheteroaryl pyrrolylindoles, as shown in Scheme 2, the scale-up annulation reaction with 1 mmol substrate **1a** was carried out under standard reaction conditions, and product **2a** was easily accessible with high yield and maintained good enantioselectivity (96% yield, 95 : 5 er). In addition, compound **2a** could undergo a condensation–cyclization reaction with 2,2-diethoxy-*N*,*N*-dimethylethan-1-amine to furnish product **3** containing an indolo[3,2-*a*]carbazole skeleton in 80% yield without erosion of the er value, which forms the key core structure in natural indolo[3,2-*a*]carbazole alkaloids from deep-water sponges of the genus *Asteropus*.[11]

Investigation of biological activities

In view of N–N atropisomers being core units in some natural products and bioactive molecules, we are interested in the potential biological activities of these new axially chiral *N*,*N*′-pyrrolylindoles. Consequently, the preliminary cytotoxic effects

of randomly selected *N*,*N*′-pyrrolylindole products (**2a**, *ent*-**2a**, **2b**, **2o**, **2i** and **2k**) and transformation products (**3** and *ent*-**3**) with an indolo[3,2-*a*]carbazole skeleton were then examined against some kinds of cancer cell lines, such as HL-60 cancer cells, A549 lung carcinoma cells, SMMC-7721 hepatoma cells, MDA-MB-231 breast adenocarcinoma cells, and SW480 colon cancer cells by MTS assay (MTS, 3-(4,5-dimethylthiazol-2-yl)-5(3-carboxymethoxy-phenyl)-2-(4-sulfopheny)-2H-tetrazolium). As shown in Fig. 1a, preliminary evaluation of the results showed that these structurally-important molecules generally showed a high cell inhibitory rate against these cancer cells at a concentration of 40 μM. Then, we turned our attention to testing the corresponding cytotoxicity with half maximal inhibitory concentration (IC_{50}) values of these three molecules in the low micromolar range, with the widely used anticancer drug cisplatin used as a comparison group (Fig. 1b). It is worth noting that compounds **2a** and **2i** exhibited impressive cytotoxicity against these five kinds of cancer cells with low IC_{50} values, which were generally better than the drug cisplatin. Compound **3** also showed favorable anticancer activities against A549 lung carcinoma cells, SMMC-7721 hepatoma cells and MDA-MB-231 breast adenocarcinoma cells. The distinctive preliminary results of these high-value axially chiral *N*,*N*′-pyrrolylindoles could to some extent provide potentiality in the drug discovery and development process.

Mechanistic studies

Having established the synthesis of axially chiral *N*,*N*′-pyrrolylindoles based on *o*-alkynylanilines *via de novo* indole formation, we were interested in the reaction mechanism. To explore the mechanistic insights for this protocol, as depicted in Scheme 3a, further investigations and control experiments were then carried out. Substrates **1w** and **1x** without an indole group and the N–Bn protected substrate **1y** did not work under

Table 2 Substrate scope of *N*-pyrrolo-acetylanilines[a]

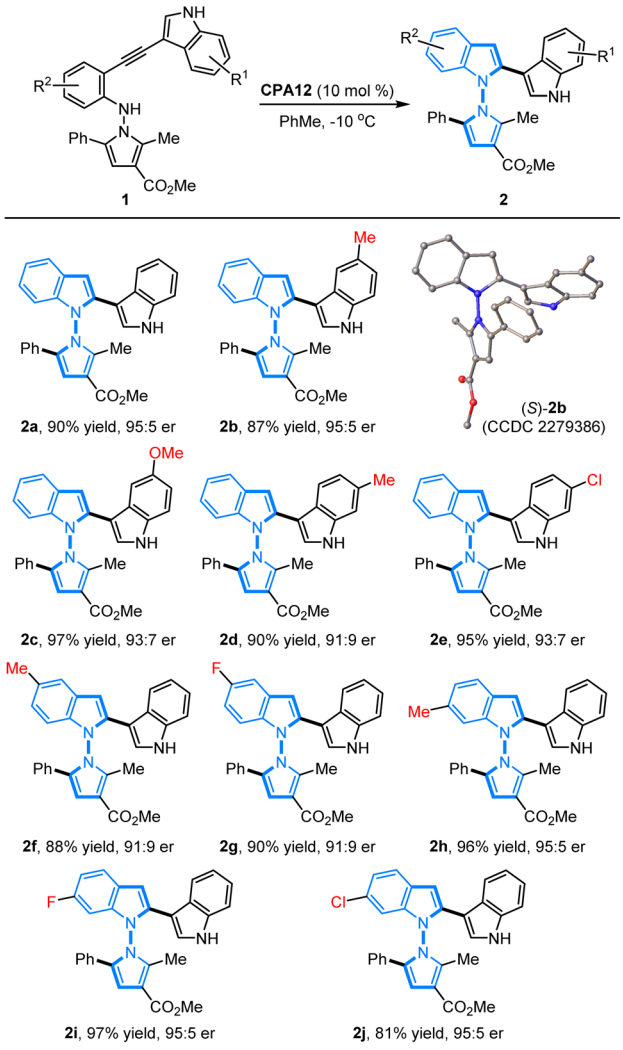

[a] All reactions were carried out with 0.2 mmol **1** in 2 mL of toluene catalyzed by **CPA12** (10 mol%) at −10 °C. The yield is isolated yield. The er value was determined by chiral HPLC analysis.

Table 3 Substrate scope of *N*-pyrrolo-acetylanilines[a]

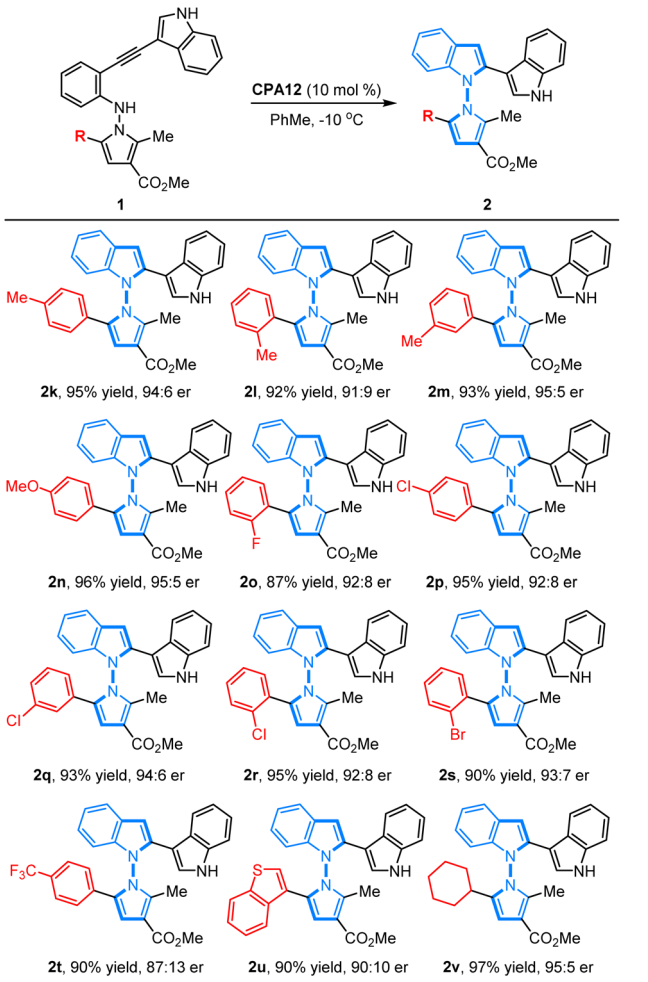

[a] All reactions were carried out with 0.2 mmol **1** in 2 mL of toluene catalyzed by **CPA12** (10 mol%) at −10 °C. The yield is isolated yield. The er value was determined by chiral HPLC analysis.

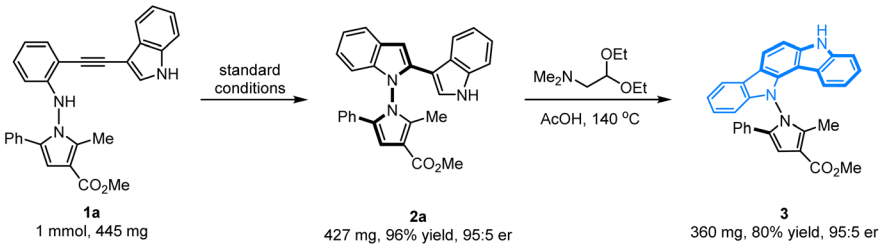

Scheme 2 Scale-up experiment and synthetic transformation.

standard reaction conditions, leading to there being no desired product, which indicated that the indole group must be involved in the reaction pathway. In addition, substrate **1z** in the absence of an ester group was also utilized to give the desired product **2z** in 79% yield with 72% ee, which demonstrated that the ester group may play an important role in determining stereoselective control (Scheme 3b). Then, we paid attention to an investigation of the nonlinear effect between the enantioselectivity of **2a** and the ee value of the **CPA12** catalyst. As shown in Scheme 3c, linear correlation was observed, indicating that one active catalyst species was involved in the stereodetermination process.

To gain mechanistic insights into the CPA-dependent stereoselectivity, density functional theory (DFT) calculations were performed with the Gaussian 09 package.[12] As shown in Fig. 2a, the reaction starts with the hydrophosphoryloxylation of the alkyne moiety in the CPA-substrate adduct **IM1** *via* **TS1** with an energy barrier of 16.9 kcal mol^{-1}, leading to allene-type intermediate **IM2**.[13] Subsequently, the nucleophilic cyclization of the N atom in the aniline moiety on the central carbon of the allene moiety occurs *via* **TS2** ($\Delta G^{\ddagger}$ = 21.3 kcal mol^{-1}), forming protonated indole complex **IM3**. Finally, the deprotonation *via* **TS3** delivers product **2a** and regenerates **IM1** through product/substrate exchange. Herein, the transition state of proton transfer **TS3** could not be located, which may be because proton transfer from ammonium to the phosphate anion could be regarded as an extremely facile process (see ESI† for more details). Overall, *N*-nucleophilic cyclization *via* **TS2** is the rate-

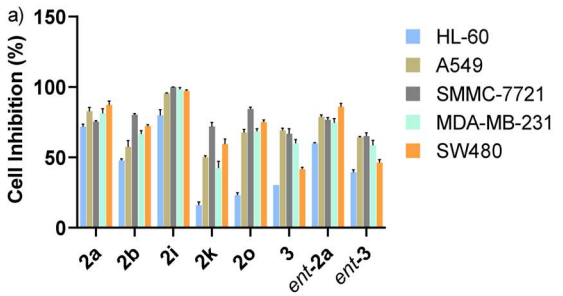

b)

	IC50 (μM)			
	2a	**2i**	**3**	cisplatin
HL-60	17.36± 0.37	11.72± 0.42	-	10.25± 0.73
A549	6.79± 0.22	10.15± 0.38	13.89± 1.37	25.03± 1.40
SMMC-7721	13.45± 0.94	11.35± 0.51	20.90± 1.85	23.86± 1.49
MDA-MB-231	18.22± 1.11	12.58± 0.49	23.57± 0.74	21.31± 1.74
SW480	15.91± 0.75	12.41± 0.53	-	19.95± 1.71

Fig. 1 (a) 40 μM of eight randomly selected chiral *N*,*N*′-pyrrolylindoles were incubated individually with HL-60 cancer cells, A549 lung carcinoma cells, SMMC-7721 hepatoma cells, MDA-MB-231 breast adenocarcinoma cells, and SW480 colon cancer cells. (b) The cell viability after incubation with different concentrations of three chiral *N*,*N*′-pyrrolylindoles and their IC_{50} values were determined in comparison to cisplatin.

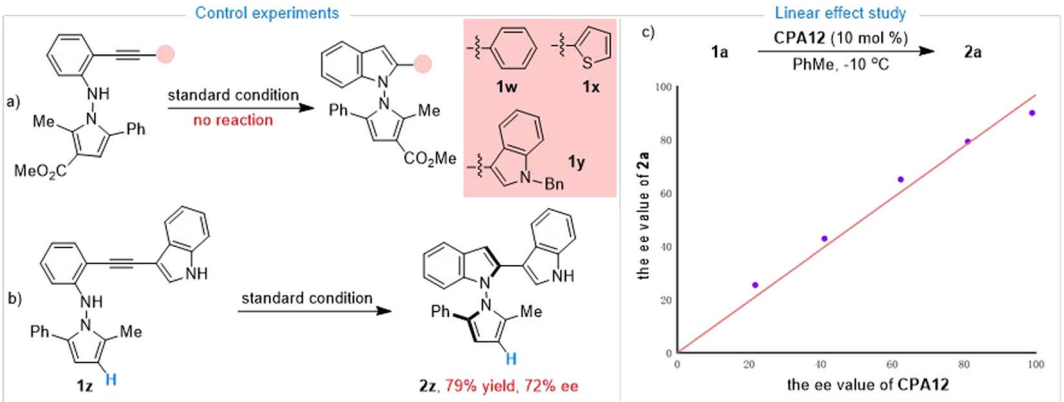

Scheme 3 Control experiments and linear effect study.

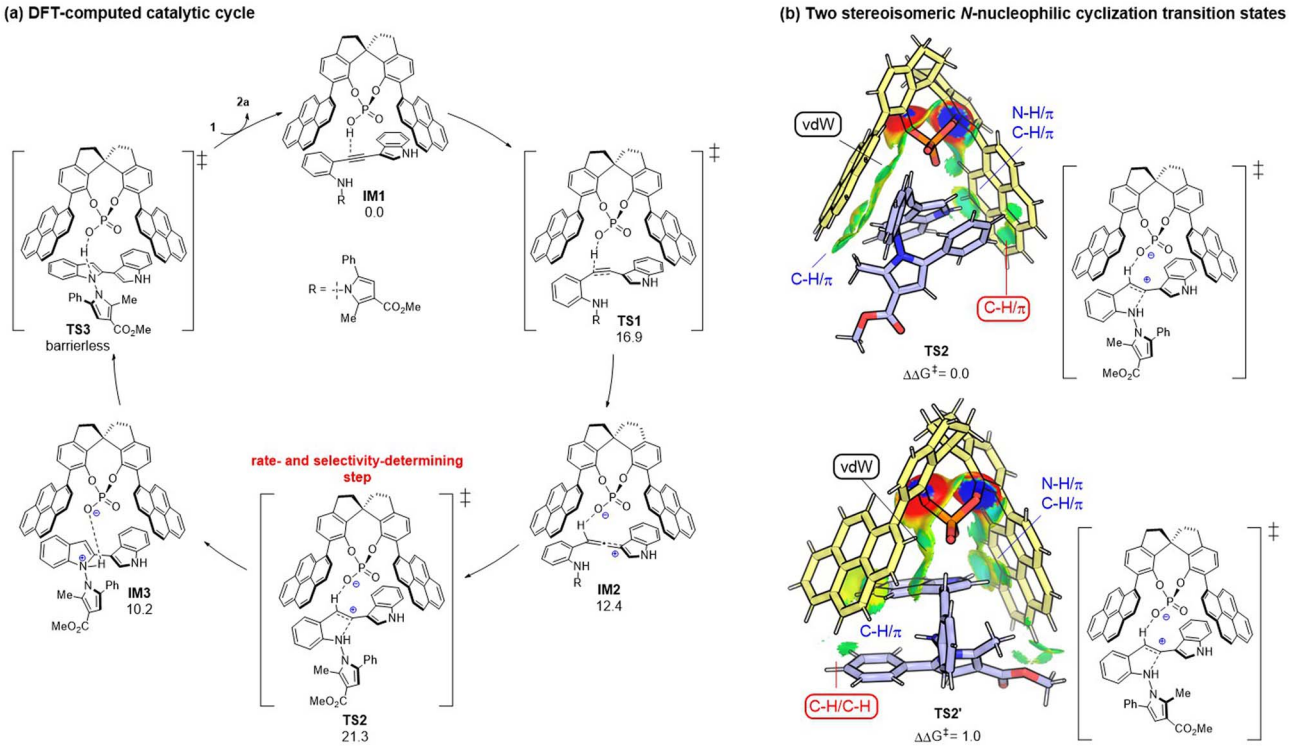

Fig. 2 (a) DFT-computed catalytic cycle with free energy given in kcal mol^{-1}. (b) Origin of the stereoselectivity between **TS2** and **TS2′**. Comparison of key NCIs by IGMH analysis.

and stereo-determining step that controls the axial chirality of the formed product. **TS2** (leading to the major product) is found to be lower than **TS2′** (leading to the minor product) by 1.0 kcal mol^{-1}, whose computed result agrees with the experimental observations. Noncovalent interactions (NCIs) using IGMH analysis have been utilized to compare the two competing transition states (**TS2** *vs.* **TS2′**).[14] As shown in Fig. 2b, the main difference between the two transition states is that **TS2** has favorable C–H···π dispersion interactions between the phenyl group of the pyrrole moiety and the pyrenyl substituent in CPA; while only weak C–H/C–H ligand–substrate interactions can be detected in **TS2′** of the analogous parts. Accordingly, the ligand–substrate dispersion interactions serve as the key factor controlling the axial chirality of the *N*,*N*′-pyrrolylindole products.

Conclusions

In summary, we developed the first organocatalytic atroposelective synthesis of axially chiral *N*,*N*′-pyrrolylindoles based on *o*-alkynylanilines through CPA-catalyzed asymmetric 5-*endo-dig* cyclization *via de novo* indole formation. This elegant protocol provided a facile synthetic strategy, and a broad range of intriguing *N*,*N*′-pyrrolylindoles were obtained in high yields with exclusive regioselectivity and excellent atroposelectivities (up to 99% yield, >20 : 1 rr, 95 : 5 er). The scale-up synthesis and the synthetic transformation for the construction of an indolo[3,2-*a*]carbazole skeleton as a key core structure in natural product asteropusazoles exhibited potential utilization. Preliminary studies of biological activity suggested that these structurally important *N*,*N*′-pyrrolylindoles had a low IC_{50} value, which could offer an encouraging opportunity for drug discovery. DFT mechanistic explorations indicated that the stereochemistry was regulated by the CPA-promoted *N*-nucleophilic cyclization step, wherein the favored transition state is stabilized by more ligand–substrate C–H···π dispersion forces.

Data availability

All experimental procedures, characterisation data, mechanistic investigations, NMR spectra and HPLC spectra can be found in the ESI.†

Author contributions

C. J. W. conceptualized the project. C. J. W. and X. Q. D. supervised the investigation. C. S. W., Q. X., and H. R. Y. performed the research. Y. D. directed the DFT calculation, and H. X. performed the DFT calculation research. C. J. W., X. Q. D. and Y. D. co-wrote the paper. All authors analyzed the data, discussed the results, and commented on the manuscript.

Conflicts of interest

There are no conflicts to declare.

Acknowledgements

This work was supported by NSFC (22071186, 22071187, 22073067, 22101216, 22271226, and 22371216), National Youth Talent Support Program, Hubei Province NSF (2020CFA036 and 2021CFA069), and Fundamental Research Funds for the Central Universities (2042022kf1180). The authors thank Dr Ran Zhang from the Core Facility of Wuhan University for his generous support in the X-ray structures analysis.

Notes and references

1 (*a*) P. Antognazza, T. Benincori, S. Mazzoli, F. Sannicolo and T. Pilati, *Phosphorus Sulfur*, 1999, **144**, 405–408; (*b*) M. Shoeb, S. Celik, M. Jaspars, Y. Kumarasamy, S. M. MacManus, L. Nahar, P. K. Thoo-Lin and S. D. Sarker, *Tetrahedron*, 2005, **61**, 9001–9006; (*c*) X.-Y. Liu, Y.-L. Zhang, X. Fei, L.-S. Liao and J. Fan, *Chem. - Eur. J.*, 2019, **25**, 4501–4508.

2 (*a*) J. Wencel-Delord, A. Panossian, F. R. Leroux and F. Colobert, *Chem. Soc. Rev.*, 2015, **44**, 3418–3430; (*b*) B. Zilate, A. Castrogiovanni and C. Sparr, *ACS Catal.*, 2018, **8**, 2981–2988; (*c*) T.-Z. Li, S.-J. Liu, W. Tan and F. Shi, *Chem.–Eur. J.*, 2020, **26**, 15779–15792; (*d*) J. K. Cheng, S.-H. Xiang, S. Li, L. Ye and B. Tan, *Chem. Rev.*, 2021, **121**, 4805–4902; (*e*) X.-F. Bai, Y.-M. Cui, J. Cao and L.-W. Xu, *Acc. Chem. Res.*, 2022, **55**, 2545–2561; (*f*) J. K. Cheng, S.-H. Xiang and B. Tan, *Acc. Chem. Res.*, 2022, **55**, 2920–2937; (*g*) P. Rodríguez-Salamanca, R. Fernández, V. Hornillos and J. M. Lassaletta, *Chem.–Eur. J.*, 2022, **28**, e202104442; (*h*) J. S. Sweet and P. C. Knipe, *Synthesis*, 2022, **54**, 2119–2132; (*i*) Y.-J. Wu, G. Liao and B.-F. Shi, *Green Synth. Catal.*, 2022, **3**, 117–136; (*j*) H.-H. Zhang and F. Shi, *Acc. Chem. Res.*, 2022, **55**, 2562–2580; (*k*) G. Bringmann, A. J. Price Mortimer, P. A. Keller, M. J. Gresser, J. Garner and M. Breuning, *Angew. Chem., Int. Ed.*, 2005, **44**, 5384–5427; (*l*) E. Kumarasamy, R. Raghunathan, M. P. Sibi and J. Sivaguru, *Chem. Rev.*, 2015, **115**, 11239–11300; (*m*) G. Ma and M. P. Sibi, *Chem.—Eur. J.*, 2015, **21**, 11644–11657; (*n*) D. Bonne and J. Rodriguez, *Chem. Commun.*, 2017, **53**, 12385–12393; (*o*) Y.-B. Wang and B. Tan, *Acc. Chem. Res.*, 2018, **51**, 534–547; (*p*) S. Zhang, G. Liao and B. Shi, *Chinese J. Org. Chem.*, 2019, **39**, 1522–1528; (*q*) Z. Li and S. Yu, *Sci. Sin.: Chim.*, 2020, **50**, 509–525; (*r*) J. A. Carmona, C. Rodríguez-Franco, R. Fernández, V. Hornillos and J. M. Lassaletta, *Chem. Soc. Rev.*, 2021, **50**, 2968–2983; (*s*) B.-C. Da, S.-H. Xiang, S. Li and B. Tan, *Chin. J. Chem.*, 2021, **39**, 1787–1796; (*t*) C.-X. Liu, W.-W. Zhang, S.-Y. Yin, Q. Gu and S.-L. You, *J. Am. Chem. Soc.*, 2021, **143**, 14025–14040; (*u*) G.-J. Mei, W. L. Koay, C.-Y. Guan and Y. Lu, *Chem*, 2022, **8**, 1855–1893.

3 C. Chang and R. Adams, *J. Am. Chem. Soc.*, 1931, **53**, 2353–2357.

4 (*a*) W. Lin, Q. Zhao, Y. Li, M. Pan, C. Yang, G. H. Yang and X. Li, *Chem. Sci.*, 2021, **13**, 141–148; (*b*) G.-J. Mei, J. J. Wong, W. Zheng, A. A. Nangia, K. N. Houk and Y. Lu, *Chem*, 2021, **7**, 2743–2757; (*c*) M. Pan, Y. B. Shao, Q. Zhao and X. Li, *Org. Lett.*, 2022, **24**, 374–378; (*d*) C. Portolani, G. Centonze, S. Luciani, A. Pellegrini, P. Righi, A. Mazzanti, A. Ciogli, A. Sorato and G. Bencivenni, *Angew. Chem., Int. Ed.*, 2022, **61**, e202209895.

5 (*a*) X.-M. Wang, P. Zhang, Q. Xu, C.-Q. Guo, D.-B. Zhang, C.-J. Lu and R.-R. Liu, *J. Am. Chem. Soc.*, 2021, **143**, 15005–15010; (*b*) Q. Xu, H. Zhang, F.-B. Ge, X.-M. Wang, P. Zhang, C.-J. Lu and R.-R. Liu, *Org. Lett.*, 2022, **24**, 3138–3143; (*c*) W. Yao, C.-J. Lu, L.-W. Zhan, Y. Wu, J. Feng and R.-R. Liu, *Angew. Chem., Int. Ed.*, 2023, **62**, e202218871; (*d*) S.-Y. Yin, Q. Zhou, C.-X. Liu, Q. Gu and S.-L. You, *Angew. Chem., Int. Ed.*, 2023, **62**, e202305067.

6 (*a*) K.-W. Chen, Z.-H. Chen, S. Yang, S.-F. Wu, Y.-C. Zhang and F. Shi, *Angew. Chem., Int. Ed.*, 2022, **61**, e202116829; (*b*) Y. Gao, L. Y. Wang, T. Zhang, B. M. Yang and Y. Zhao, *Angew. Chem., Int. Ed.*, 2022, **61**, e202200371.

7 L.-Y. Pu, Y.-J. Zhang, W. Liu and F. Teng, *Chem. Commun.*, 2022, **58**, 13131–13134.

8 (*a*) P. Zhang, Q. Xu, X.-M. Wang, J. Feng, C.-J. Lu, Y. Li and R.-R. Liu, *Angew. Chem., Int. Ed.*, 2022, **61**, e202212101; (*b*) Z.-H. Chen, T.-Z. Li, N.-Y. Wang, X.-F. Ma, S.-F. Ni, Y.-C. Zhang and F. Shi, *Angew. Chem., Int. Ed.*, 2023, **62**, e202300419.

9 (*a*) N. Ototake, Y. Morimoto, A. Mokuya, H. Fukaya, Y. Shida and O. Kitagawa, *Chem. - Eur. J.*, 2010, **16**, 6752–6755; (*b*) Y. Morimoto, S. Shimizu, A. Mokuya, N. Ototake, A. Saito and O. Kitagawa, *Tetrahedron*, 2016, **72**, 5221–5229; (*c*) L. Peng, K. Li, C. Xie, S. Li, D. Xu, W. Qin and H. Yan, *Angew. Chem., Int. Ed.*, 2019, **58**, 17199–17204; (*d*) Z.-S. Wang, L.-J. Zhu, C.-T. Li, B.-Y. Liu, X. Hong and L.-W. Ye, *Angew. Chem., Int. Ed.*, 2022, **61**, e202201436; (*e*) M. Tian, D. Bai, G. Zheng, J. Chang and X. Li, *J. Am. Chem. Soc.*, 2019, **141**, 9527–9532; (*f*) Y.-P. He, H. Wu, Q. Wang and J. Zhu, *Angew. Chem., Int. Ed.*, 2020, **59**, 2105–2109; (*g*) X. Li, L. Zhao, Z. Qi and X. Li, *Org. Lett.*, 2021, **23**, 5901–5905; (*h*) C.-S. Wang, L. Wei, C. Fu, X.-H. Wang and C.-J. Wang, *Org. Lett.*, 2021, **23**, 7401–7406; (*i*) W.-C. Yang, X.-B. Chen, K.-L. Song, B. Wu, W.-E. Gan, Z.-J. Zheng, J. Cao and L.-W. Xu, *Org. Lett.*, 2021, **23**, 1309–1314; (*j*) V. Hutskalova and C. Sparr, *Synthesis*, 2023, **55**, 1770–1782; (*k*) L. Yu, J. Liu, S. Xiang, T. Lu, P. Ma and Q. Zhao, *Org. Lett.*, 2023, **25**, 522–527.

10 CCDC 2279386 ((*S*)-**2b**) contains the supplementary crystallographic data for this paper.

11 (*a*) F. Russell, D. Harmody, P. J. McCarthy, S. A. Pomponi and A. E. Wright, *J. Nat. Prod.*, 2013, **76**, 1989–1992; (*b*) X. Zheng, L. Lv, S. Lu, W. Wang and Z. Li, *Org. Lett.*, 2014, **16**, 5156–5159.

12 DFT studies were conducted at the M06-2X/def2-TZVP(SMD)//M06-2X/6-31G** level. See ESI† for computational details.

13 Y.-B. Wang, P. Yu, Z.-P. Zhou, J. Zhang, J. Wang, S.-H. Luo, Q.-S. Gu, K. N. Houk and B. Tan, *Nat. Catal.*, 2019, **2**, 504–513.

14 (*a*) S. Grimme, *Angew. Chem., Int. Ed.*, 2008, **47**, 3430–3434; (*b*) A. J. Neel, M. J. Hilton, M. S. Sigman and F. D. Toste, *Nature*, 2017, **543**, 637–646.